CIRRELT

Centre interuniversitaire de recherche
sur les réseaux d'entreprise, la logistique et le transport

Interuniversity Research Centre
on Enterprise Networks, Logistics and Transportation

Time-Dependent Vehicle Routing Problem with Emission and Cost Minimization Considering Dynamic Paths

Hamza Heni
Jacques Renaud
Leandro C. Coelho

February 2018

CIRRELT-2018-14

Document de travail également publié par la Faculté des sciences de l'administration de l'Université Laval, sous le numéro FSA-2018-011.

Bureaux de Montréal :
Université de Montréal
Pavillon André-Aisenstadt
C.P. 6128, succursale Centre-ville
Montréal (Québec)
Canada H3C 3J7
Téléphone : 514 343-7575
Télécopie : 514 343-7121

Bureaux de Québec :
Université Laval
Pavillon Palasis-Prince
2325, de la Terrasse, bureau 2642
Québec (Québec)
Canada G1V 0A6
Téléphone : 418 656-2073
Télécopie : 418 656-2624

www.cirrelt.ca

Time-Dependent Vehicle Routing Problem with Emission and Cost Minimization Considering Dynamic Paths

Hamza Heni*, Jacques Renaud, Leandro C. Coelho

Interuniversity Research Centre on Enterprise Networks, Logistics and Transportation (CIRRELT) and Department of Operations and Decision Systems, 2325 de la Terrasse, Université Laval, Québec, Canada G1V 0A6

Abstract. The Time-dependent Vehicle Routing Problem with Emission and Cost Minimization considering Dynamic Paths consists of routing a fleet of vehicles to serve a set of customers across a time-dependent network modeled as a multigraph in which the traveling speed of each arc changes over time. The problem involves determining time-dependent paths minimizing travel time, greenhouse gas emissions, or costs to visit all customers taking into account the instantaneous speed imposed by traffic on each road segment of the underlying network. To solve the problem we propose an efficient nearest neighbor improvement heuristic that incorporates a time-dependent quickest path method. The proposed method involves the fast computation of time-dependent point-to-point paths based on different measures such as time, fuel consumption, or cost on a multigraph representing large road networks using a time-dependent label-setting algorithm. Based on new large-scale benchmark instances that realistically represent typical freight distribution operations and capture congested periods using real-life road networks and large data sets of speed observations, extensive computational experiments are conducted under three optimization criteria, namely minimizing travel time, emissions and total costs. We also carry out sensitivity analysis to assess the effects of departure time choice, congestion avoidance decisions and customer demands on the resulting routing plans. Our method significantly outperforms the results obtained with a classical heuristic based on speed limits without regard to traffic congestion.

Keywords. Time-dependent vehicle routing, greenhouse gas emissions, traffic congestion, time-dependent quickest path, multigraph.

Acknowledgements. This research was partly supported by grants 2014-05764 and 0172633 from the Natural Sciences and Engineering Research Council of Canada (NSERC) and by the Centre d'Innovation en Logistique et Chaîne d'Approvisionnement Durable (CILCAD). We also thank Mr Jean-Philippe Gagliardi, President of Logix Operations Inc., for providing us with real data from an important wholesaler partner in Québec city. This support is highly appreciated.

---

* Corresponding author: hamza.heni@cirrelt.ca

Dépôt légal – Bibliothèque et Archives nationales du Québec
Bibliothèque et Archives Canada, 2018

1 Introduction

In most countries freight transportation in urban areas is among the largest sources of greenhouse gas (GHG) emissions [Demir et al., 2014b]. With increasing road transportation activity and the expected growth of freight flows at a fast rate, GHG emissions are expected to continue to increase at a similar pace [Transports Canada, 2017]. In Canada, the transportation sector (including passenger, freight and off-road emissions) is the second-largest source of GHG, reaching 24% of the country's GHG emissions [Transports Canada, 2017].

Large urban areas continue to face congestion due to increased flow of trucks. It is widely recognized that in urban areas, vehicles must often travel at the speed imposed by traffic, which affects travel times at certain periods of the day. The variability of traveling speed has a significant impact on the performance of road freight transportation operations, GHG emissions and fuel consumption [Bektaş and Laporte, 2011]. Third-party logistics (3PL) providers are nowadays in position to acquire the speed of traffic on the road. Considering time-varying speeds and alternative paths between customers in route planning may lead to effective routes and schedules that avoid congestion, minimize GHG emissions and yield cost savings more than the traditional vehicle routing problem (VRP).

A feature largely overseen in VRPs is that between any pair of customer nodes (see Figure 1) there are many links (road segments) connecting them through the underlying physical road network (Figure 2), corresponding to multiple time-dependent paths of different travel times, costs and emissions according to time-varying speeds. Hence, routing decisions involve not only sequencing the customers but also path choices depending on departure times, customer demands and the optimization criteria. The main objective is to minimize the sum of operational and environmental costs while respecting capacity constraints. Travel cost is defined with respect to fuel consumption costs and driver wages. Moreover, when a vehicle travels across an arc it emits a certain amount of GHG which is directly proportional to the amount of fuel consumed [Franceschetti et al., 2013]. The fuel consumption depends on several factors, such as carried load, speed, road characteristics, among others. The corresponding problem is a Time-dependent Vehicle Routing Problem with Emission and Cost Minimization considering Dynamic Paths (TDVRP-ECMDP) on time-dependent networks where the flow speed of each road link depends on the time. Vehicles must travel at the speed imposed by traffic, which is determined by congestion.

Path selection in time-dependent VRPs (TDVRP) has been considered by few works. Ehmke et al. [2016b] and Qian and Eglese [2016] solved the TDVRP considering emissions-minimized paths using

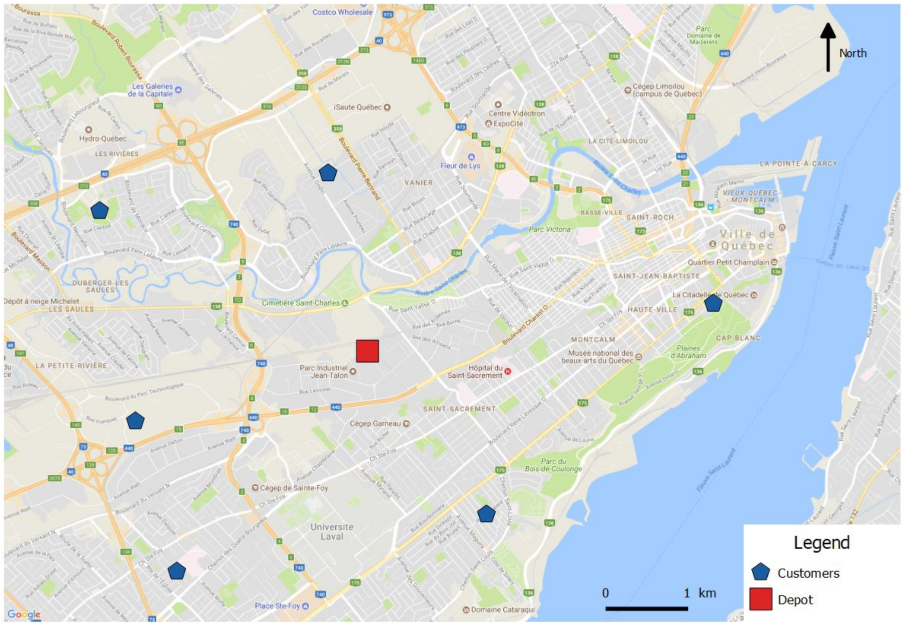

Figure 1: Illustration of a classical simplified network

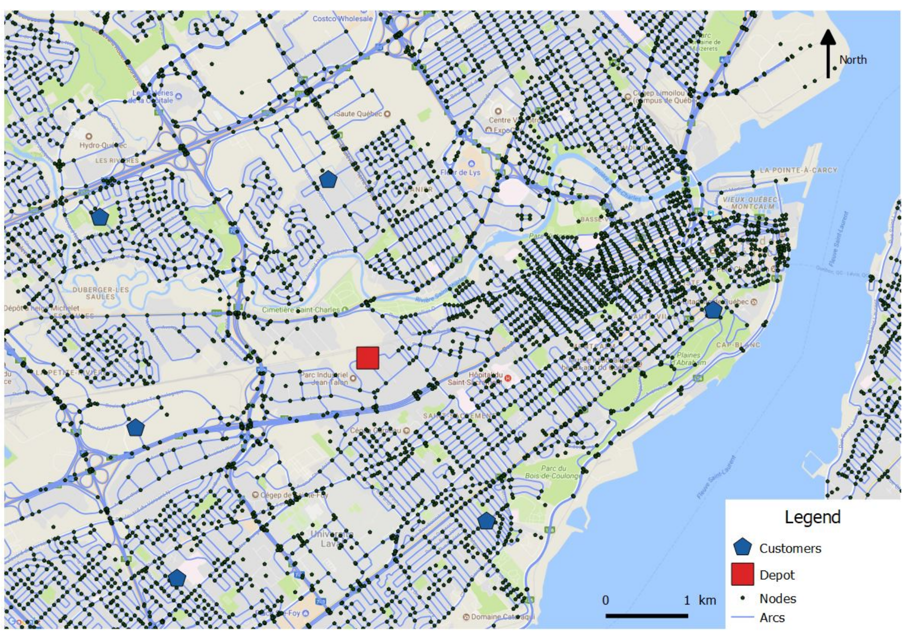

Figure 2: Illustration of a subset of customers and segment nodes of the road network of Quebec City

a tabu search and their instances was limited to 30 and 60 customers, respectively as the search space increases drastically. Huang et al. [2017] considered path flexibility in the TDVRP with a multigraph through the integration of path selection decision according to departure time and congestion levels. A multigraph model was first introduced by Garaix et al. [2010] to consider alternative paths between all pairs of key-locations. Letchford et al. [2014], Lai et al. [2016] and Ticha et al. [2017] used the multigraph representation to solve different VRPs. Their results indicate that the multigraph structure significantly increases computing times. We follow these studies by applying speed-up techniques to efficiently find appropriate time-dependent paths connecting the clients without computing them in advance for very large instances (up to 500 customers), road network (50376 arcs) and number of time slots (buckets of 15 minutes). We compute time-dependent quickest and least emission paths, and use the TD least costly path to investigate the insights related to different optimization objectives. To solve the TDVRP-ECMDP we develop efficient heuristics which are successfully applied to large road networks using a realistic set of large scale benchmark instances from 24 millions speed observations collected by furniture and appliance stores in Quebec City. We conduct sensitivity analysis to shed light on the trade-offs between multiple performance indicators, including driving time, GHG emissions and generalized costs pertaining to fuel consumption, traffic congestion, and drivers costs. Our detailed experimental analysis also quantifies the effects of flexible departure times from the depot and carried load according to customer demands. The scientific contributions of this research are fourfold:

(i) we model the underlying road network using a multigraph, which involves not only the best sequences of nodes across routes but also the fast computation of TD point-to-point quickest paths (TDQP), least emission paths (TDLEP) and least costly paths (TDLCP);

(ii) we create a new large sized benchmark set of instances reflecting real road freight distribution operations and congested areas of the road network from a large data set of speed observations;

(iii) we propose an efficient TD nearest neighbor method adapted to the multigraph representation to solve the TDVRP-ECMDP taking into account the effects of path choice and congestion avoidance decisions on GHG emissions as well as on traveling cost. Significant saving are obtained by integrating TDLCPs into routing decisions, which captures and minimizes fuel consumption along with operational costs;

(iv) we conduct sensitvity analysis to demonstrate that significant saving in terms of emissions and cost is achieved with regard to departure times.

The remainder of this paper is organized as follows. Section 2 summarizes the relevant literature. Section 3 formally describes the TDVRP-ECMDP. In Section 4, a detailed description of the designed TDVRP-ECMDP heuristics is provided. Section 5 presents extensive computational experiments and their numerical results. Finally, conclusions are stated in Section 6.

2 Literature review

In this section, we review the existing contributions on green logistics that consider the impact of GHG emissions in addition to operational issues on vehicle routing models in Section 2.1. Then, we look at existing studies on TD routing in Section 2.2.

2.1 Green logistics problems

Figliozzi [2011] studied a variant of the VRP in which GHG emissions minimization is pursued. He shows the effects of travel time optimization and the location of the depot in reducing emission levels considering scenarios with and without congestion. Likewise, Jabali et al. [2012] presented a variant of the problem with time-varying traffic. The planning horizon is divided into two periods, the first one is a congested period, whereas the second one considers free-flow.

Moreover, some have considered speed optimization decisions when dealing with emission minimization, as introduced by Bektaş and Laporte [2011]. Their model computes the travel cost through a function encompassing fuel consumption, GHG emissions and driver costs. Later, Demir et al. [2014a] introduced the bi-objective PRP in order to analyze trade-offs between fuel consumption and travel time. The authors developed a solution method based on the Adaptive Large Neighborhood Search and the speed optimization algorithm proposed by Demir et al. [2012]. They show that there is no need to greatly compromise on driving time in order to achieve a significant reduction in fuel consumption and GHG emissions. In a subsequent work, Kramer et al. [2015b] propose a solution method for the PRP combining a local search with an integer programming approach over a set covering formulation and a recursive speed optimization algorithm. This work was extended by Kramer et al. [2015a] to account for the effects of flexible departure times from the depot.

In their studies, Franceschetti et al. [2013] extend the PRP by capturing traffic congestion in the network. The authors consider three time periods: one congested, a transient one, and a free-flow period. They define conditions under which it is optimal to wait at certain nodes of the network in order to avoid congestion and to reduce GHG emissions. Later, Franceschetti et al. [2017] developed a metaheuristic to solve the PRP with time-varying traffic congestion, which uses a departure time and speed optimization procedure designed by Franceschetti et al. [2013]. In a related study, Xiao and Konak [2016] extend the PRP with time-varying traffic congestion by considering a heterogeneous vehicle fleet. In order to avoid traffic congestion and reduce emissions they designed an algorithm that allows waiting at customers and on the road. Otherwise, Dabia et al. [2017] developed an exact method based on branch-and-price to solve a variant of the PRP in which the speed decision is taken at the route level and is assumed to be the constant along a route. Recently, Behnke and Kirschstein [2017] investigate the effects of path selection on a real world network. They show that considering emission-minimizing paths between customers can lead to additional emission savings.

2.2 Time-dependent routing

Most of the literature in this field relies on the speed model of Ichoua et al. [2003], where they do not assume a constant speed over the entire length of an arc. Thus, the speed on each arc may change when the boundary between two consecutive time intervals is crossed. In this way, this model guarantees the first-in, first-out (FIFO) property [Ghiani and Guerriero, 2014b]. Another contribution in the context of FIFO dynamics is due to Van Woensel et al. [2008] who proposed a queueing approach to model traffic congestion by tacking into account the change on travel speeds. For a relevant literature review on the TD routing problems, the reader is referred to Gendreau et al. [2015].

Another research stream has focused on the link travel time model (LTM) [Delling and Nannicini, 2012] in which arc travel times are specified upon entrance to an arc and are assumed to be fixed during its traversal. In the LTM, the network does not satisfy the FIFO property, which requires additional algorithmic steps to ensure FIFO dynamics. To model travel times Fleischmann et al. [2004] proposed a smoothed travel time function satisfying the FIFO consistency.

Focusing on TD networks Sung et al. [2000] introduced the flow speed model (FSM) for a TD shortest path where the flow speed of each arc depends on the time intervals. The FSM is consistent to the FIFO property. Another recent work by Kok et al. [2012] investigated the impact of traffic congestion on the performance of vehicle route plans. The authors evaluated multiple strategies for avoiding traffic congestion when solving shortest path and VRPs. They designed a speed model to reflect the key elements of peak hour congestion on urban area networks. To solve the TDVRP they applied a modified Dijkstra algorithm and a dynamic programming heuristic.

Slightly different from the VRP, some have worked on the paths connecting two customers. Ghiani and Guerriero [2014a] and Calogiuri et al. [2015] studied the TD quickest path problem, which aims to find the least time path. They developed a TD lower bound on the time-to-target that can be computed by ignoring congestion ratios. Many studies have dealt with emission-minimizing paths between customers in vehicle routing [Ehmke et al., 2016a, Qian and Eglese, 2016, Wen et al., 2014]. These applied the Methodology for Estimating Emissions from Transport (MEET) [Hickman et al., 1999] to calculate GHG emissions which does not explicitly take the changing weight of the carried load into account. Ehmke et al. [2016b] proposed an emissions-minimizing model that explicitly accounts for the path finding problem between stops. The majority of paths between customers are pre-computed in advance using path averaging and approximation method. However, none of these works considered the effects of flexible departure times or waiting at depot and traffic conditions on both emissions and costs.

Finally, some related work on TD routing have focused on the optimization of routing plans by explicitly considering path flexibility [Androutsopoulos and Zografos, 2017, Ehmke et al., 2016b, Huang et al., 2017, Qian and Eglese, 2016]. They also indicate that path flexibility increases the problem size requiring efficient heuristics to solve large scale instances. Although Ehmke et al. [2016b] and Qian and Eglese [2016] use finer speed levels to depict the 24 hour traffic conditions, the planing horizon in their instances usually contains only one peak hour or daily period. Even if the benefits of both GHG emissions and costs saving in vehicle routing and scheduling are clear, there is a lack of research on the TDVRP with cost minimization considering TDLCP computation which considers time-varying speeds for each road segment across a road network, and not only for customer links. The only works we are aware of that focused in finding TDLCPs are those of Wen et al. [2014], Di Bartolomeo et al. [2017] and Heni et al. [2017]. Hence, this paper focus on solving large scale instances and deals explicitly with the trade-off between travel time, fuel consumption and cost in TDVRP involving emission and cost optimization considering time-varying speeds, congestion and dynamic paths on the underlying networks.

3 Problem description

The TDVRP-ECMDP is defined on a network (multigraph) $\mathcal{G}^{\mathcal{T}} = (\mathcal{V}^{\mathcal{T}}, \mathcal{A}^{\mathcal{T}}, \mathcal{Z}^{\mathcal{T}})$ in which $\mathcal{V}^{\mathcal{T}} = \mathcal{V} \cup \mathcal{V}^{g} \cup \{0\}$ is the set of all nodes: the depot is represented by node 0, the set of customer nodes is $\mathcal{V}$, and the set $\mathcal{V}^{g}$ represents the other nodes of the road networks. $\mathcal{A}^{\mathcal{T}} = \{(u, v) : u, v \in \mathcal{V}^{\mathcal{T}}, u \neq v\}$ is the sparse set of all road segments connecting pair of nodes of the network, some of them being customers. Let $\mathcal{T} = z_0 + \mathcal{H}\delta$ be the length of the planning horizon within which all routes must be completed, where $\delta > 0$ represents the smallest increment of time over which a change in the speed happens. This planning horizon is divided into a finite number $\mathcal{H}$ of time intervals $\mathcal{Z}_h = [z_0 + h\delta, z_0 + (h+1)\delta[$ considering the set $\mathcal{Z}^{\mathcal{T}} = \{z_0, z_0 + \delta ..., z_0 + \mathcal{H}\delta\}$ of discrete times, with $h = 0, 1, 2, ..., \mathcal{H} - 1$. With each road segment $(u, v) \in \mathcal{A}^{\mathcal{T}}$ is associated a time-dependent travel speed s_{uv}^h during time interval $\mathcal{Z}_h$. In particular, based on the FSM we assume that the speed of each road segment varies as the time interval changes. Thus, when a vehicle travels across a road segment (u, v), its traveling speed is not constant over the full arc, but may change when the boundary between two consecutive time intervals is crossed. Hence, the speed s_{uv}^h on arc (u, v) is assumed to be constant over a given time interval $\mathcal{Z}_h$ and can be defined as:

$$s_{uv}^h = \sigma_{uv}^h \mathcal{U}_{uv}, \tag{1}$$

where $\sigma_{uv}^h \in [0, 1]$ represents the congestion factor of arc (u, v) during the time interval $\mathcal{Z}_h$ and $\mathcal{U}_{uv}$ is the speed limit imposed by traffic regulations.

For any road segment $(u, v) \in \mathcal{A}^{\mathcal{T}}$ let L_{uv} denote the distance between nodes u and v. Let l_{uv}^h represent the portion of the length L_{uv} covered during time interval $\mathcal{Z}_h$. Let h_t and h_γ be the indices of time intervals where the start time t at node u and the arrival time $\gamma_v^p(t)$ at node v belong to, respectively, with $h_t \in \{0, ..., \mathcal{H} - 1\}$ and $h_\gamma \in \{h_t, ..., \mathcal{H} - 1\}$. Let $\tau_{uv}(t)$, $f_{uv}(t)$ and $c_{uv}(t)$ be the travel time, amount of GHG emissions and travel cost, respectively, related to the time $t \in \mathcal{T}$ at which a vehicle leaves node u to node v. The travel time function is piecewise linear and satisfies the FIFO property:

$$\tau_{uv}(t) = \sum_{h=h_t}^{h_\gamma} l_{uv}^h / s_{uv}^h. \tag{2}$$

Furthermore, a homogeneous fleet of vehicles with capacity $\mathcal{Q}$ is available at the depot. Each customer $i \in \mathcal{V}$ has a non-negative demand q_i and a service time w_i, $q_0 = w_0 = 0$. We denote the set of customers included in route r as $\mathcal{V}(r) \subseteq \mathcal{V}$. Let $\gamma_i^p(t)$ be a function that provides the ready time at node i when service is fulfilled given a starting time t at the depot. Let Ω_{ij} be the set of all feasible paths on $\mathcal{G}^{\mathcal{T}}$ connecting any pair of depot and customers nodes i, j through the underlying road network. Each path $p_{ij} \in \Omega_{ij}$ is composed of an ordered sequence of nodes $[i, \langle u_{ij}^0, ..., u_{ij}^n \rangle, j]$. Considering that the road segments attributes are TD, travel time, fuel consumption and travel cost between a pair of customers is defined by a dynamic path that varies according to the departure time, which is defined by the schedule of traversing it as $p_{ij}(\gamma_i(t)) = (\gamma_i(t), [i, \langle u_{ij}^0, ..., u_{ij}^n \rangle, j])$. Any scheduled route r must follow an ordered sequence of node, and pair of nodes being connected by dynamic paths, such as TDLCPs, on the multigraph:

$$\Psi_r(t) = (v_0, p_{01}(\gamma_0(t)), \ldots, p_{k-1,k}(\gamma_{k-1}(t)), v_k), \tag{3}$$

where $v_k \in \mathcal{V} \cup \{0\}$, $v_0 = v_k = 0$, $u_{k-1,k}^m \in \mathcal{V}^{\mathcal{T}}$ are road segment extremities, and k represents the number of stops on the complete route.

The aim of the TDVRP-ECMDP is to construct a set of feasible routes that meet the demand of all customers without split delivery, starting and ending at the depot, driving at the speed of the traffic without exceeding the vehicle capacity nor violating their workday duration, so as to minimize a travel cost function encompassing the cost of driver's wage, fuel consumption, and GHG emissions.

3.1 Modeling GHG emissions

Following relevant works in the literature (e.g., Ehmke et al. [2016b], Huang et al. [2017]) we consider the comprehensive modal emissions model (CMEM) [Barth and Boriboonsomsin, 2008, 2009] to calculate fuel consumption for heavy duty vehicles. Based on the CMEM with a given speed s, total vehicle weight $\mathcal{M}^p$ across a given path p_{ij} and road gradient θ the resulting instantaneous fuel consumption rate (in $liters/second$) is computed as follows:

$$e_r = \mathcal{E}_0 \left(\mathcal{E}_1 + \left(\frac{(\alpha \mathcal{M}^p + \beta s^2)s}{\mathcal{E}_2} + \mathcal{P}_{acc} \right) \right), \tag{4}$$

where $\mathcal{E}_0 = \frac{\zeta}{\varpi \psi}$, $\mathcal{E}_1 = kN_eV$, $\mathcal{E}_2 = \frac{1}{\varepsilon 1000 \eta_{tf}}$, $\mathcal{M}^p = \omega + q_i$, $\alpha = a + g \sin\theta + gC_r \cos\theta$, $\beta = 0.5C_dA\rho$, and $\mathcal{P}_{acc}$ are constant parameters related to the vehicle and its engine. All parameter values used are provided in A.

Moreover, considering only the average speed one may not capture precise GHG emissions. For example, if the travel speed on a road segment often drops far below the average speed during a specific time slot $\mathcal{Z}_h$, then the actual emissions will be much higher than if the trip occurs consistently at the average speed. Thus, to optimize GHG emissions in an urban area, we must explicitly consider the variability of the speed at different times of the day. Hence, for a given path p_{ij} traversed by a vehicle departing from customer i at ready time $\gamma_i^p(t)$, the corresponding fuel consumption (in $liters$)

can be computed as follows:

$$\mathcal{F}_{p_{ij}}(t) = \sum_{(u,v)\in p_{ij}} f_{uv}(\gamma_u^p(t)), \tag{5}$$

where

$$\gamma_u^p(t) = \begin{cases} t & \text{if } u = 0 \\ \gamma_{u-1}^p(t) + \tau_{u-1,u}(\gamma_{u-1}^p(t)) & \text{if } u \in \mathcal{V}^g \\ \gamma_{u-1}^p(t) + \tau_{u-1,u}(\gamma_{u-1}^p(t)) + w_u & \text{if } u \in \mathcal{V}, \end{cases} \tag{6}$$

and $f_{uv}(t) = f_{uv}^1(t) + f_{uv}^2(t) + f_{uv}^3(t)$. The first term f^1 denotes the fuel consumption related to the vehicle weight, f^2 represents the fuel consumption implied by travel time, and component f^3 measures the fuel consumption incurred by the variations in speed:

$$f_{uv}^1(t) = \sum_{h=h_t}^{h_\gamma} \left[\left(\frac{l_{uv}^h}{s_{uv}^h} \right) \frac{\alpha \mathcal{M}^p \mathcal{E}_0}{\mathcal{E}_2} s_{uv}^h \right] = \frac{\alpha \mathcal{M}^p \mathcal{E}_0}{\mathcal{E}_2} \sum_{h=h_t}^{h_\gamma} l_{uv}^h = \frac{\alpha \mathcal{M}^p \mathcal{E}_0}{\mathcal{E}_2} L_{uv}, \tag{7}$$

$$f_{uv}^2(t) = \sum_{h=h_t}^{h_\gamma} \left[\left(\frac{l_{uv}^h}{s_{uv}^h} \right) \mathcal{E}_0 \mathcal{E}_1 \right] = \mathcal{E}_0 \mathcal{E}_1 \tau_{uv}(t), \tag{8}$$

$$f_{uv}^3(t) = \sum_{h=h_t}^{h_\gamma} \left[\left(\frac{l_{uv}^h}{s_{uv}^h} \right) \frac{\beta \mathcal{E}_0}{\mathcal{E}_2} (s_{uv}^h)^3 \right] = \frac{\beta \mathcal{E}_0}{\mathcal{E}_2} \sum_{h=h_t}^{h_\gamma} \left[l_{uv}^h . (s_{uv}^h)^2 \right]. \tag{9}$$

3.2 Modeling travel costs

In this section, we model the TD travel cost of a particular path. Given a departure time t, the driver cost incurred from path p_{ij} can be simply computed by multiplying the sum of the traveling time across road segments connecting customers nodes (i, j) by the driver wage c_d:

$$\mathcal{C}(\Gamma_{p_{ij}}(t)) = c_d \sum_{(u,v)\in p_{ij}} \tau_{uv}(\gamma_u^p(t)). \tag{10}$$

The cost of fuel consumption for a given route r can be computed by multiplying the fuel consumption

(5) by a factor c_e representing the price of a liter of fuel:

$$\mathcal{C}(\mathcal{F}_{p_{ij}}(t)) = c_e \sum_{(u,v)\in p_{ij}} f_{uv}(\gamma_u^p(t)). \tag{11}$$

The path cost encompasses the path duration and fuel costs:

$$\mathcal{C}_{p_{ij}}(t) = c_d \sum_{(u,v)\in p_{ij}} \tau_{uv}(\gamma_u^p(t)) + c_e \sum_{(u,v)\in p_{ij}} f_{uv}(\gamma_u^p(t)). \tag{12}$$

4 Heuristic methods for the TDVRP-ECMDP

With respect to exact methods, solving large VRP instances using a multigraph representation of the underlying road network increases significantly the size of the solution space as shown by Garaix et al. [2010] and Letchford et al. [2014] for VRPs, and Huang et al. [2017] for TDVRP with path flexibility. Even with heuristic approaches, Ehmke et al. [2016b] solved TDVRP with emissions minimizing paths limited to 30 customers and one-hour time intervals due to computation time. Hence, to efficiently solve large instances of the TDVRP-ECMDP considering time-varying speeds we propose two solution methods. The first one only considers the speed limits on the underlying road network. The second method takes traffic congestion into account by considering time-varying speeds of all transportation links between each pair of customer nodes. The proposed heuristic methods are followed by a TD neighborhood search improvement heuristic (TDNSIH) to enhance the solution by using intra- and inter-route exchanges.

4.1 Static nearest neighbor heuristic

The static nearest neighbor heuristic (SNNH) does not take traffic congestion into account and solves the TDVRP-ECMDP considering static scenarios where the paths between customers are fixed. Thus, it works only on the customer network considering speed limits. The static paths used by the SNNH are chosen with respect to the optimization objective by solving the corresponding point-to-point routing problem, namely the Quickest Path Problem (QPP), the Least Emission Path Problem (LEPP) or the Least Cost Path Problem (LCPP). The SNNH begins each route by determining, from the set of remaining customers, the unrouted customer to be visited next having the least additional increase in the objective function. When the search fails to find unrouted customers who can feasibly be embedded to the end of a route, the heuristics starts a new one.

4.2 Time-dependent nearest neighbor heuristic

To solve the TDVRP-ECMDP we also propose a greedy heuristic that accounts for traffic congestion and dynamic paths. The TD nearest neighbor heuristic (TDNNH) solves the problem according to three variants of TD point-to-point routing problems: TDQPP, TDLEPP and TDLCPP. The proposed heuristics considers the multigraph $\mathcal{G}^{\mathcal{T}}$ to construct the set of routes. Table 1 shows the notation used to develop the TDNNH.

Table 1: Additional notation used by the TDNNH

Notation	Description
$\mathcal{E}^{\mathcal{T}}$	Set of processed nodes
$\mathcal{N}^{\mathcal{T}}$	Set of remaining nodes
$\mathcal{N}^{c}$	Set of remaining customer nodes
$\mathcal{E}^{\mathcal{T}}_{+}(u)$	Set of successor nodes of node u
Ψ_r	Ordered set of customers visited along a route r
$\Psi_{\mathcal{R}}$	Set of feasible routes

The TDNNH is briefly introduced in the following algorithmic steps (see Algorithm 1). The heuristic starts a time-dependent goal-directed search from the depot. The TDNNH takes into consideration the closeness of the customer node to be examined. The closeness is an estimated goal cost defined based on different measures such as fuel consumption, travel time or cost. At each iteration if the active labeled node having the smallest cost is a customer, then we check if the customer could be added to the current route with respect to the time window associated with the depot and the capacity of the vehicle, otherwise a new route is started. Then, we begin again a new time-dependent goal directed search from the current customer node. The heuristic stops when all customer nodes are processed.

The travel cost of each road link is computed according to the entering time on the arc and to the flow speed at the time of traversing it. The physical network is used to find connecting paths between each pair of nodes in the global network. Algorithm 2 is used to compute fuel consumption, travel time and travel cost for a given road segment. Given a starting time $\gamma^{p}_{u}(t)$ at node u, the fuel consumption, GHG emissions and travel costs across arc (u, v) are computed using the FSM based on Algorithm 2. At each covered time period the time-dependent flow speed is identified and the length of the appropriate portion of the distance L_{uv} is calculated. Hence, at every iteration the time-dependent

Algorithm 1 Determination of a TDVRP-ECMDP solution using the TD quickest path method (TDNNH)

$\Psi_{\mathcal{R}} \leftarrow \emptyset,\ \mathcal{N}^c \leftarrow \mathcal{V}$
function TDNNH($\Psi_{\mathcal{R}}, \mathcal{N}^c, \mathcal{G}^{\mathcal{T}}, t$)
    $\mathcal{E}^{\mathcal{T}} \leftarrow \varnothing,\ \mathcal{N}^{\mathcal{T}} \leftarrow \mathcal{V}^{\mathcal{T}},\ r \leftarrow |\Psi_{\mathcal{R}}|,\ \gamma \leftarrow t,\ c_o \leftarrow 0,\ predecessor(o) \leftarrow 0,\ c_u \leftarrow \infty | \tau_u \leftarrow 0,\ \forall u \in \mathcal{V}^{\mathcal{T}}$
    while $|\mathcal{E}^{\mathcal{T}}| < |\mathcal{V}^{\mathcal{T}}|$ or $|\mathcal{N}^c| = 0$ **do**
        let $u \in \mathcal{N}^{\mathcal{T}} | c_u \leftarrow \min\{c_v : v \in \mathcal{N}^{\mathcal{T}}\}$
        $\mathcal{E}^{\mathcal{T}} \leftarrow \mathcal{E}^{\mathcal{T}} \cup \{u\},\ \mathcal{N}^{\mathcal{T}} \leftarrow \mathcal{N}^{\mathcal{T}} \setminus \{u\}$
        if $u \in \mathcal{N}^c$ **then**
            $\gamma \leftarrow (\gamma + \tau_u + w_u)$
            if $\Psi = \emptyset$ **then**
                Step 1:
                $\Psi_r \leftarrow \Psi_r \cup \{(u, o)\},\ \Psi_{\mathcal{R}} \leftarrow \Psi_{\mathcal{R}} \cup \Psi_r\ ,\ \mathcal{N}^c \leftarrow \mathcal{N}^c \setminus \{u\},\ r \leftarrow r + 1$
                Start a new route: $TDNNH(\Psi_{\mathcal{R}}, \mathcal{N}^c, \mathcal{G}^{\mathcal{T}}, t)$
                if $\mathcal{N}^c = \emptyset$ **then**
                    return $\Psi_{\mathcal{R}}$
                else
                    Go to Step 2
                end if
            else
                $\Gamma_{p_{uo}} \leftarrow TD\_Dijkstra(u, o, \gamma, \mathcal{G}^{\mathcal{T}})$
                if u can be added to current route r **then**
                    $\Psi_r \leftarrow \Psi_r \cup \{(u, v)\},\ \mathcal{N}^c \leftarrow \mathcal{N}^c \setminus \{u\}$
                    Go to Step 2
                else
                    Go to Step 1
                end if
            end if
        end if
        Step 2:
        $\gamma \leftarrow \gamma + \tau_u$
        for each $(u, v) \in \mathcal{E}^{\mathcal{T}}_{+}(u)$ **do**
            if $c_v > \left[TD\_Cost\_FSM(\gamma, (u, v), \mathcal{Z}^{\mathcal{T}})) \longrightarrow c_{uv}(\gamma)\right]$ **then**
                $c_v \leftarrow c_u + \left[TD\_Cost\_FSM(\gamma, (u, v), \mathcal{Z}^{\mathcal{T}})) \longrightarrow c_{uv}(\gamma)\right]$
                $\tau_v \leftarrow \tau_u + \left[TD\_Cost\_FSM(\gamma, (u, v), \mathcal{Z}^{\mathcal{T}})) \longrightarrow \tau_{uv}(\gamma)\right]$
                $predecessor(v) \leftarrow u$
            end if
        end for
    end while
end function

travel cost and fuel consumption are calculated. The algorithm stops when node v is reached.

When performing time restriction validation the TDNNH involves the fast computation of point-to-point TD quickest path, least emission path or least cost path in a time-dependent network using an efficient TD Dijkstra (TD-Dijkstra) label-setting algorithm (see B) based on Brodal and Jacob [2004] and Dean [2004]. Note that, finding the TDLCP is NP-Hard as stated by Dehne et al. [2012] and demonstrated by Di Bartolomeo et al. [2017]. To reduce the computational time our adaptation on the algorithm maintains a single label for each node including travel time, fuel and cost information.

Algorithm 2 Computing TD travel time, fuel consumption and cost across a given road segment (u, v) according to the FSM

function TD_COST_FSM($\gamma_u^p(t)$, (u, v), $\mathcal{Z}^{\mathcal{T}}$)
  $h | \gamma_u^p(t) \in Z_h = [z_h, z_{h+1}[$
  $k \leftarrow h$, $d \leftarrow L_{uv} - s^k_{uv}(z_{k+1} - \gamma_u^p(t))$
  $l \leftarrow s^k_{uv}(z_{k+1} - \gamma_u^p(t))$
  $g \leftarrow kN_eV\left(\frac{l}{s^k_{uv}}\right) + l\lambda\varsigma\beta(s^k_{uv})^2$
  while $d > 0$ **do**
    $k \leftarrow k + 1$, $l \leftarrow \delta s^k_{uv}$, $d \leftarrow d - l$
    $g \leftarrow g + \mathcal{E}_0\mathcal{E}_1\left(\frac{l}{s^k_{uv}}\right) + l\frac{\beta\mathcal{E}_0}{\mathcal{E}_2}(s^k_{uv})^2$
  end while
  $\gamma_v^p(t) \leftarrow z_{k+1} + d/s^k_{uv}$
  if $k > h$ **then**
    $l \leftarrow s^k_{uv}(\gamma_v^p(t) - z_k)$
    $g \leftarrow g + \mathcal{E}_0\mathcal{E}_1\left(\frac{l}{s^k_{uv}}\right) + l\frac{\beta\mathcal{E}_0}{\mathcal{E}_2}(s^k_{uv})^2$
  else
    $g \leftarrow \mathcal{E}_0\mathcal{E}_1\left(\frac{l}{s^k_{uv}}\right) + l\frac{\beta\mathcal{E}_0}{\mathcal{E}_2}(s^k_{uv})^2$
  end if
  $\tau_{uv}(\gamma_u^p(t)) \leftarrow \gamma_v^p(t) - t$
  $f_{uv}(\gamma_u^p(t)) \leftarrow \frac{\alpha\mathcal{M}\mathcal{E}_0}{\mathcal{E}_2}L_{uv} + g$
  $c_{uv}(\gamma_u^p(t)) \leftarrow c_d\tau_{uv}(\gamma_u^p(t)) + c_e f_{uv}(\gamma_u^p(t)$
   return $\left[\tau_{uv}(\gamma_u^p(t)), f_{uv}(\gamma_u^p(t)), c_{uv}(\gamma_u^p(t))\right]$
end function

4.3 Time-dependent nearest neighborh and improvement heuristic

The main components of local search heuristics are the rules applied to generate the neighboring solutions employed to carry out the exploration of the solution space and identify the best neighbor solution. In the TDNSIH, the neighborhoods are constructed by applying efficient implementations of arc-exchange algorithms. Exchanges are performed by replacing some arcs by new ones and moving them within the same route. Note that any modification in a route may need a major recalculation of the paths linking two consecutive customers, starting from the point of modification of the route up to the return to the depot.

The appropriate arc-exchange neighborhoods are defined successively based on six operators commonly applied in the literature (e.g., Zachariadis and Kiranoudis [2010]):

(i) 1-0-Exchange: iteratively removes a node and reinserts it at its best position.

(ii) 1-1-Exchange: the position of customer i is exchanged with that of customer j that yields the largest decrease in cost.

(iii) Or-Opt: sequences of one to three consecutive nodes are moved. This results in replacing up to three arcs in the original route by three new one.

(iv) Intra-2-Opt: tries to improve each route separately by exchanging a pair of arcs. If an improvement is possible, the two arcs that yield the largest decrease in objective value are removed and the resulting paths are reconnected in the reverse order.

(v) Inter-2-Opt*: tries to merge two routes. The first route is simply followed by the second one. The new route, if feasible, has one fewer arc.

(vi) Inter-CROSS-Exchange: is performed by removing two arcs for a first route as well as two arcs from a second route. Then the customers are swapped by introducing new arcs that yields the smallest detour [Taillard et al., 1997]. Note that the orientation of both routes is preserved.

The general structure of the designed TDNSIH is summarized in Algorithm 3. At each iteration, once a potential neighboring solution is determined at the first neighborhood, it is compared against the current solution $\Psi_{\mathcal{R}}$. If the new neighboring solution is better, it becomes the current solution, and the exploration of the current neighborhood continues. If no better solution is found through the exploration of the first neighborhood, the TDNSIH starts the search in the second neighborhood. If a better solution is determined, the heuristic goes back to explore the first neighborhood. Otherwise, the TDNSIH selects the next predefined neighborhood $Neighbor_k$ and looks for further improvement of the current solution. The TDNSIH stops if no better solution is found on the set of established neighborhoods.

A new neighbor solution is generated only if the deadline restriction is not exceeded. For inter-route moves new routes are generated with respect to vehicle capacity constraints. The evaluation of each neighbor solution implies the calculation of cost change and the validation of deadline through the fast computation of point-to-point TD paths connecting the new sequence of customers of each updated route on the underlying physical transportation network using a TD-Dijkstra algorithm. In the case in which deadline is not exceeded, we update the cost of each arc using the appropriate TDQP, TDLEP or TDLCP.

Algorithm 3 Time-dependent neighborhood search improvement heuristic (TDNSIH)

function TD_NSIH($\Psi_{\mathcal{R}}, \mathcal{G}^{\mathcal{T}}$)
  $nb\_max\_neighbors \leftarrow 6$, $improve \leftarrow 1$, $k \leftarrow 1$
  while $improve = 1$ **do**
    $\Psi_{\mathcal{R}'} \leftarrow Neighbor_k(\Psi_{\mathcal{R}})$, $improve \leftarrow 0$
    if $\mathcal{C}(\Psi_{\mathcal{R}'}) < \mathcal{C}(\Psi_{\mathcal{R}})$ **then**
      $\Psi_{\mathcal{R}} \leftarrow \Psi_{\mathcal{R}'}$, $k \leftarrow 1$, $improve \leftarrow 1$
    else
      if $k < nb\_max\_neighbors$ **then**
        $k \leftarrow k + 1$, $improve \leftarrow 1$
      end if
    end if
  end while
  return $\Psi_{\mathcal{R}}$
end function

5 Computational experiments

In this section we provide the results of extensive computational experiments we have conducted to solve the TDVRP-ECMDP and to assess the performance our heuristics. We first explain how the benchmark instances are generated based on real traffic data from the road network of Québec City. We then discuss the results of our experiments. Particularly, a comparison is made between routing strategies with and without time-varying speeds to illustrate several insights concerning the impact of congestion avoidance, path choice decisions, optimization objective, departure time and volume of demand. These are measured and compared in terms of distance, travel time, fuel consumption (GHG emissions) and costs.

5.1 Proposed benchmark instances

Benchmark instances are designed using the geospatial road network covering the delivery regions of our industrial partner in Québec City. Each constructed test instance contains up to 50,376 road segments connecting 17,431 geographical nodes, the depot and customers. The speed limit of each road segment depends on the road type, namely highways, urban roads and primary roads. We have defined 56 time periods of 15 minutes from 6h00 to 21h00, which covers a typical workday. Time-varying speed data was extracted and analyzed by geomatic experts [Belhassine et al., 2018]. Hence, for each road segment and each time slot the speed is computed based on a large set of real traffic data including more than 24 million of GPS speed observations provided by our logistic partners. We used pgRouting library 2.0 and QGIS 2.18 for the geomatic developments.

As presented in Table 2, we propose three classes of instances using three variants of networks, namely, small, medium and large to take into account different shipping patterns. For each instance we consider multiple departure times (07h00, 08h00, 09h00 and 10h00) from the depot to capture the effects of congestion. Additionally, three demand scenarios (low, medium, and high) are applied to reflect the impact of load quantities on route plans. There is a total of 132 instances for the TDVRP-ECMDP.

Table 2: TDVRP-ECMDP benchmark instances

Instances	Time-dependent networks	Number of customers	Number of nodes	Number of arcs	Departure time	Demand
S1 S2 S3 S4 S5	Small network	10 20 30 40 50	1612	2810	07h00 08h00 09h00 10h00	Low Medium High
M1 M2 M3	Medium network	100 175 200	3859	5388		
L1 L3 L4	Large network	300 400 500	17431	50367		

5.2 Experimental setting

Computational experiments are carried out by applying the solution methods to assess the benefit of quickest path optimization considering time-varying speeds on the reduction of both operational and environmental costs. Our algorithms were coded in C++ 17 and OpenMP for multithreading programming using Jetbrains CLion release 2.4 and tested on a ThinkCenter workstation with 32-gigabyte RAM and Intel i7 vPro, running Ubuntu Linux 16.05 LTS x86.

Table 3 provides an overview of our experimental plan. Each of the 132 instances is solved for three different objective functions minimizing: (i) travel time using quickest paths, (ii) fuel/emission using least emission paths, and (iii) costs using least costly paths. We do this twice, first without considering traffic information using the speed limit of each arc, and then with our real-life traffic information using time-varying speeds. The solutions will then be compared in terms of their distances (Dist), travel times (TT), fuel consumption, cost, number of routes, number of late deliveries (#LD), and number of late returns to the depot (#LR), percentage gap between two solutions calculated as $100 * (Solution - Solution_{best})/Solution_{best}$, and percentage improvement between two solutions.

Table 3: Overview of experimental setting

Optimization criteria	Accounting for traffic congestion	Heuristic	Solution evaluation measure
Travel time Fuel (GHG emissions) Costs	No (speed limits)	SNNH	Distance (m) Travel time (s) Fuel consumption (liters) Cost ($) # vehicle routes # late deliveries # late return times to depot Gap (%) Improvement (%)
	Yes (time-varying speeds)	TDNNH	

5.3 Experimental results

In this section we analyze the performance of our heuristics. We will first concentrate our analysis for departure times at 08h00 with low demand. Table 4 illustrates the effect of fixed speed assumption on the accuracy of travel time, fuel consumption and cost computations, by providing the results over all benchmark instances using the classical SNNH and TDNNH according to three optimization measures. Results are obtained as follows. When an optimization measure is chosen, e.g., travel time, the SNNH algorithm is applied with the corresponding point-to-point algorithm, in this example, the quickest path one. The results, which are obtained without considering congestion, are reported in Table 4 under the columns TT, Fuel and Cost. Then, each solution is evaluated by considering congestion on each of the selected path leading to the results under the columns TD-TT, TD-Fuel and TD-Cost. If we take instance S1 as an example with the travel time as optimization objective, the associated travel time without congestion is 1900. When congestion is applied to this solution, the real travel time increases to 3104. The relative difference between the two solutions, measured as $(3104-1900)/3104$, is reported under the Gap (%) column. Table 4 shows that using the TD algorithm TDNNH for this instance yields a travel time of 2472 leading to an improvement of 20.36% which demonstrates the value of considering congestion during the resolution process.

From Table 4 we see that solutions with respect to minimization objectives show similar patterns: SNNH applied on real-world network generates a high gap between 20 and 36.47% for key evaluation metrics, namely, travel time, fuel consumption, and cost under realistic traffic congestion. For example, when applying the cost optimization objective, there is an average gap of 36.47% on travel time (15,309.18 vs 24,096.55 seconds) and 20.66% on fuel (96.43 vs 121.54 liters), leading to a gap of 30.06% on overall cost (241.00 vs 344.59$). Additionally, with the SNNH, on average, in 73.91% (2.55 out of 3.45 routes) of cases, vehicles return late to the depot. One explanation for this is the underestimation of traffic congestion effects on delays across selected paths. Hence, fixed speed calculations are not sufficiently accurate compared to TD ones, which affects the efficiency of route plans. Therefore, these results show that time-varying speeds have a strong impact on fuel consumption and cost computations.

As shown in Table 4, compared to the SNNH we observe that the TDNNH yields the best solutions over all instances under real-world networks considering time-varying speeds enabling more fuel and cost savings. When looking at the cost optimization objective, we can see that for all S*, M* and L* instances, the TDNNH produces an average travel time of 21,576.82 seconds, which is 10.46% lower than SNNH (24,096.55 seconds). Second, the fuel consumption reported by the TDNNH (under the cost objective) is 116.24 liters for a distance of 246.55 km which corresponds to 47.15 liters/100 km, which is 4.36% lower than the SNNH (121.54 liters). The obtained value is very close to the average consumption of 46.90 reported by the annual statistical report of Transports Canada [2017]. Finally, the TDNNH generates global savings on overall cost of 7.98% (317.08 instead of 344.59$). It is remarkable that the same patterns hold for travel time and fuel objectives. This exposes the error margin associated with using speed limits instead of using calculations with time-varying speeds. These results clearly show that the quality of route plans strongly increase if we consider time-varying speeds using TDNNH compared to those generated with SNNH that uses fixed speeds and that are adjusted considering traffic congestion.

Table 5 shows that our improvement heuristic TDNSIH is able to improve solutions generated by the TDNNH heuristics using the cost optimization criterion. Regarding the quality of the solution, as measured by fuel consumption reduction and cost improvements when compared to the previous solution, we see that the savings on overall costs with respect to medium demands is of up to 7.51% combined with an overall decrease of travel time by 3.54% and a reduction on fuel consumption by 6.89%. As expected the proposed TD exchange moves produce alternative paths that allow congestion avoidance yielding potential reductions of travel times, fuel consumption and costs. Note that the TDNSIH is time-consuming as it runs multiple exchange operators to improve input solutions, which requires finding and computing alternative paths on the multigraph.

Regarding the performance and scalability of the TDNNH, the results from Table 6 reported for instance with medium demand show that in terms of computational time (CPU) our heuristic is very effective even for large instances with 300-500 customers. As an example, for the travel time objective, solving 100 customer instances M1 requires only 8.08–8.80 seconds. The global average runtime over all optimization objectives vary from 17.99 to 26.38 seconds. This is due to the fact that the TDNNH applies a goal directed search based on the fast computation of point-to-point paths between customer

Table 4: Computational results of the SNNH and TDNNH for different optimization criteria

Optimization measure	Instances	SNNH													TDNNH							
		Dist	TT	TD-TT	Gap (%)	Fuel	TD-Fuel	Gap (%)	Cost	TD-Cost	Gap (%)	#Routes	#LD	#LRTD	Dist	TD-TT	Imp (%)	TD-Fuel	Imp (%)	TD-Cost	Imp (%)	#Routes
Travel Time	S1	28787.50	1900	3104	38.79	10.89	14.76	26.22	29.03	43.36	33.05	1	10	0	28992.49	2472	20.36	12.72	13.82	35.64	17.80	1
	S2	29694.17	2117	3895	45.65	11.98	17.39	31.11	31.77	53.10	40.17	1	20	0	30962.95	2933	24.70	14.65	15.76	41.78	21.32	1
	S3	39601.42	2794	4903	43.01	16.27	22.55	27.85	42.46	67.61	37.20	1	30	0	42113.26	3766	23.19	19.58	13.17	54.52	19.36	1
	S4	51468.95	3806	5249	27.49	21.49	25.93	17.12	57.07	74.43	23.32	1	40	0	59307.18	5147	1.94	25.64	-4.94	75.04	-0.82	1
	S5	61427.71	4413	6363	30.65	25.79	31.72	18.69	67.17	90.56	25.83	1	50	0	59314.43	5305	16.63	28.07	11.51	77.37	14.56	1
	M1	158886.82	10903	18117	39.82	66.63	87.79	24.10	169.30	254.95	33.59	2	100	2	164008.87	15422	14.88	79.40	9.56	222.40	12.77	3
	M2	196510.46	14327	23588	39.26	82.70	110.59	25.22	216.88	327.67	33.81	3	150	2	218106.04	20160	14.53	104.61	5.41	291.66	10.99	4
	M3	241989.70	17167	28292	39.32	101.65	134.18	24.24	262.82	394.79	33.43	4	200	3	274611.38	25329	10.47	131.70	1.85	366.76	7.10	5
	L1	504617.79	30076	42854	29.82	205.05	242.10	15.30	491.46	642.67	23.53	6	300	5	526368.51	41454	3.27	236.39	2.36	624.21	2.87	7
	L2	583468.65	35586	55162	35.49	238.12	292.31	18.54	576.32	805.04	28.41	8	400	7	623879.88	51084	7.39	284.31	2.74	761.17	5.45	9
	L3	691278.03	42872	67142	36.15	283.22	350.32	19.15	690.11	973.58	29.12	10	500	9	714542.23	58942	12.21	331.31	5.43	882.01	9.41	10
	Average	**235248.29**	15087.36	23515.36	35.84	96.71	120.88	20.00	239.49	338.89	29.33	**3.45**	163.64	2.55	249291.57	**21092.18**	10.30	**115.45**	4.49	**312.05**	7.92	3.91
Fuel Consumption	S1	27183.97	1948	3082	36.79	10.88	14.26	23.7	29.07	42.6	31.76	1	10	0	27754.5	2526	18.04	12.62	11.50	35.98	15.54	1
	S2	29603.16	2118	3920	45.97	11.97	17.45	31.40	31.76	53.39	40.51	1	20	0	30960.31	2933	25.18	14.65	16.05	41.78	21.75	1
	S3	37079.26	2761	5038	45.20	15.42	22.42	31.22	41.19	54.82	24.86	1	30	0	36824.82	3786	24.85	18.45	17.71	53.39	2.61	1
	S4	47489.11	3595	5067	29.05	20.04	24.53	18.30	53.6	71.28	24.80	1	40	0	49569.13	4857	4.14	24.28	1.04	69.20	2.92	1
	S5	56903.32	4200	5911	28.95	24.10	29.32	17.80	63.41	83.96	24.48	1	50	0	55676.97	5372	9.12	27.45	6.38	77.23	8.02	1
	M1	140865.74	10554	17339	39.13	60.61	81.12	25.28	159.42	240.67	33.76	2	100	1	161858.78	16390	5.47	81.60	-0.59	233.16	3.12	3
	M2	189060.07	14145	23083	38.72	81.20	108.28	25.01	213.63	320.73	33.39	3	150	2	199829.99	20821	9.80	102.84	5.02	295.25	7.94	4
	M3	239271.14	17681	25376	30.32	102.00	127.39	19.93	267.59	362.19	26.12	4	200	2	240960.33	24894	1.90	123.59	2.98	353.73	2.34	5
	L1	470094.37	31439	48961	35.79	195.32	246.06	20.62	491.85	699.13	29.65	6	300	5	515976.69	44620	8.87	243.06	1.22	658.79	5.77	7
	L2	556234.92	38286	60495	36.71	233.00	297.64	21.72	593.38	856.488	30.72	8	400	7	608081.81	54046	10.66	288.48	3.08	791.14	7.63	9
	L3	606845.94	41756	65138	35.90	254.89	322.66	21.00	648.05	924.73	29.92	10	500	9	679157.74	61334	5.84	324.93	-0.70	895.00	3.21	11
	Average	**218239.18**	15316.64	23946.36	36.04	91.77	117.38	21.82	235.72	337.27	30.11	**3.45**	163.64	2.36	236968.28	**21961.73**	8.29	**114.72**	2.27	**318.6**	5.54	4
Cost	S1	27728.22	1908	3076	37.97	10.89	14.38	24.27	28.73	42.69	32.70	1	10	0	28728.49	2472	19.64	12.67	11.89	35.59	16.63	1
	S2	29603.16	2118	3920	45.97	11.97	17.45	31.40	31.76	53.39	40.51	1	20	0	30960.31	2933	25.18	14.65	16.05	41.78	27.75	1
	S3	37079.26	2761	5038	45.20	15.42	22.42	31.22	41.19	68.60	39.96	1	30	0	41336.73	3766	25.25	19.41	13.43	54.33	20.80	1
	S4	51276.43	3844	5281	27.21	21.50	25.91	17.02	57.39	74.69	23.16	1	40	0	50953.14	4920	6.84	24.70	4.67	70.23	5.97	1
	S5	60293.60	4419	6306	29.92	25.45	31.18	18.38	66.83	89.45	25.29	1	50	0	58066.54	5261	16.57	27.68	11.23	76.56	14.41	1
	M1	154938.57	11243	18948	40.66	65.68	88.76	26.00	171.09	263.10	34.97	2	100	1	179326.06	16941	10.59	87.07	1.90	244.12	7.21	3
	M2	190181.47	13625	22529	39.52	79.75	106.39	25.04	207.5	313.85	33.89	3	150	2	188471.62	18441	18.15	94.17	11.49	265.05	15.55	3
	M3	239333.76	17217	28142	38.82	100.89	133.35	24.34	262.37	392.56	33.16	4	200	3	272926.74	26763	4.90	135.98	-1.97	383.86	2.22	5
	L1	525223.48	32059	49250	34.91	211.64	258.45	18.11	515.8	715.84	27.94	6	300	6	555539.51	44986	8.66	251.71	2.61	671.84	6.15	7
	L2	572652.25	35707	56047	36.29	235.81	292.53	19.39	574.69	812.81	29.30	8	400	7	611756.63	51245	8.57	281.88	3.64	759.75	6.53	9
	L3	678845.67	43500	66525	34.61	281.69	346.08	18.61	693.70	963.46	28.00	10	500	9	693992.86	59617	10.38	328.73	5.01	884.78	8.17	11
	Average	**233377.81**	15309.18	24096.55	36.47	96.43	121.54	20.66	241.00	344.59	30.06	**3.45**	163.64	2.55	246550.78	**21576.82**	10.46	**116.24**	4.36	**317.08**	7.98	3.91

Table 5: Computational results of the designed TDNSIH according to the cost optimization criterion

Demand	Instances	TDNSIH									
		Dist	%Imp Dist	TT	%Imp TT	Fuel	%Imp Fuel	Cost	%Imp Cost	#Routes	CPU
Low	S1	28728.49	0.00	2472	0.00	12.67	0.00	35.59	0.00	1	39.04
	S2	30638.77	1.04	2915	0.61	14.54	0.75	41.49	0.69	1	767.77
	S3	35850.53	13.27	3403	9.64	17.24	11.18	48.75	10.47	1	3069.89
	S4	48941.98	3.95	4578	6.95	23.34	5.51	65.75	6.38	1	10763.90
	S5	55820.61	3.87	5058	3.86	26.62	3.38	73.61	3.85	1	12397.93
	Average	39996.08	4.43	3685.20	4.21	18.88	4.16	53.04	4.29	1	5407.71
Medium	S1	28778.85	0.00	2470	0.00	13.09	0.00	36.05	0.00	1	74.00
	S2	45679.38	0.06	4324	2.74	21.96	1.92	62.01	2.41	2	767.77
	S3	48001.51	7.47	4544	8.22	23.43	7.72	65.56	8.02	2	3069.89
	S4	57131.20	1.43	5717	2.26	22.66	21.75	63.76	23.20	3	1184.31
	S5	72972.21	1.03	6744	4.49	34.68	3.07	97.21	3.90	3	950.06
	Average	50512.63	2.00	4759.80	3.54	23.16	6.89	64.92	7.51	2.20	1209.21
High	S1	42236.93	0.00	3733	0.00	19.65	0.00	54.32	0.00	2	55.27
	S2	47077.27	1.05	4486	0.04	22.72	0.39	64.26	0.14	3	767.77
	S3	68510.51	2.03	6422	2.07	33.16	2.01	92.73	2.03	4	3069.89
	S4	90856.53	4.73	8467	6.16	43.95	5.00	122.51	5.69	6	527.79
	S5	108855.57	0.70	10347	1.15	53.23	0.95	149.16	1.07	7	715.48
	Average	71507.36	1.70	6691	1.88	34.54	1.67	96.60	1.79	4.40	1027.24

nodes.

To further assess the impacts of traffic congestion on travel time, fuel consumption and cost, the results from Table 6 show solutions according to departure times first at 07h00 with medium demand. Note that the results of the time-independent SNNH are not reported as fixed speed calculations are incoherent with the following analysis. Globally, we note that in most cases the TDNNH produces coherent results with respect to the optimization objective. As expected, when the fuel consumption minimization criterion is applied, the obtained values of fuel consumption (160.66, 165.06, 165.59 and 161.11 liters when starting at 07h00, 08h00, 09h00 and 10h00, respectively) is lower than the values generated by those obtained when optimizing time. The same pattern holds for cost minimization criterion. From these results we can conclude that minimizing the travel time does not minimize the fuel consumption in such environments.

Regarding the cost minimization criterion, we can see from Table 6 that the travel cost is effectively lower with respect to its value when compared against the other minimization criteria, as expected. For the case of 07h00 departure, we notice that the cost minimization objective requires less travel time that when minimizing fuel consumption (27989.27 instead of 28806.55 seconds) but an increase in distance (349729.57 instead of 343220.52 meters), yielding a small reduction in the overall cost by 1.64% (422.56 instead of 429.61$). The same observation holds for the other departure times. This pattern is not observed in the other optimization criteria.

From Table 6 we also see that delayed departure times can lead to higher fuel consumption. When looking at the cost minimization criteria we observe that fuel consumption increases on average, by

3.56% (160.57 at 07h00 versus 166.29 liters at 08h00), combined with an increase in travel time of up to 6.34% (27989.27 at 07h00 versus 29764.09 seconds at 08h00), leading to a global fluctuation on overall costs of 5.13% (422.56 at 07h00 versus 444.22$ at 08h00). We observe that allowing flexible departures can lead to better route plans using alternative paths yielding fuel and cost savings.

Additional experiments were performed to study the impact of delayed departure time and rush hours traffic congestion on key performance metrics. Figure 3 shows in more details the impact of flexible departure times on fuel consumption and total costs for a 100 customers instance with medium demands. In Figure 3, the results of the TDNNH according to 28 departure times between 06h00 and 14h00 replicate the traffic pattern of Québec City with a moderate morning congestion between 06h00 and 07h45. Then, congestion rapidly increases between 07h45 and 09h15. Between 09h30 and 11h00 drivers face a low traffic congestion leading to lower fuel consumption. Hence, all customers can be served with less fuel and costs when starting between 06h00 and 07h45 or 09h30 and 11h00 compared to other periods. In the afternoon congestion impacts traffic between 13h00 and 13h30 leading to much higher fuel consumption. Interestingly, we observe that even with the same number of vehicles (6 routes for all departure times) congestion has a considerable impact on fuel consumption. These results clearly show that allowing delayed or flexible departures may lead to better alternative paths by avoiding traffic congestion yielding better route plans that lead to the reduction of GHG emissions and savings on overall costs.

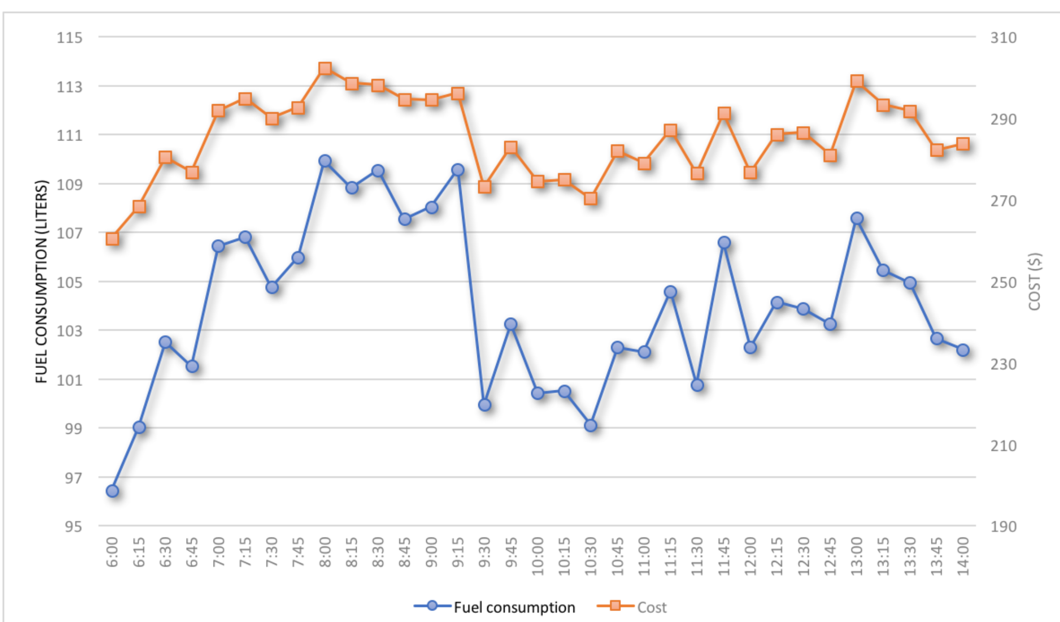

Figure 3: Effects of flexible departure times on fuel consumption and costs considering 100 customers with medium demand

Table 6: Impacts of departure time on the emissions of alternative routes: average using the TDNNH for different optimization criteria

Optimization measure	Instances	07h00						08h00						09h00						10h00					
		Dist	TT	Fuel	Cost	#Routes	CPU	Dist	TT	Fuel	Cost	#Routes	CPU	Dist	TT	Fuel	Cost	#Routes	CPU	Dist	TT	Fuel	Cost	#Routes	CPU
Travel Time	S1	30479.42	2470	13.565	36.60	1	0.48	29259.33	2470	13.17	36.14	1	0.48	29515	2636	13.83	38.31	1	0.529	29899.12	2596	13.87	38.01	1	0.48
	S2	45183.64	3964	20.91	57.74	2	0.98	40001.63	3517	18.713	51.42	2	0.86	45966.38	4384	22.25	62.85	2	0.90	40765.36	3661	19.38	53.41	2	0.87
	S3	53283.55	4734	25.03	69.018	2	1.24	50780.25	4719	24.45	68.22	2	1.191	53516.93	5034	26.025	72.72	2	1.223	51015.77	4790	24.753	69.18	2	1.23
	S4	67197.60	5782	30.47	84.19	3	1.83	65390.99	6224	31.49	89.11	3	1.575	69985.27	6292	32.68	91.07	3	1.639	60796.34	5861	29.44	83.68	3	1.55
	S5	77563.11	7049	36.56	101.96	3	2.10	76327.99	7247	36.84	103.96	3	1.96	75196.50	6983	36.00	100.76	3	1.99	77551.74	7038	36.77	102.10	3	2.07
	M1	218023.12	19486	104.75	286.10	6	8.29	214312.95	19193	103.14	281.75	6	8.98	228573.44	19522	107.25	289.28	6	8.24	224089.17	19319	105.57	285.62	6	8.80
	M2	276466.88	23781	130.25	351.92	8	12.66	288301.37	25403	137.85	374.45	8	13.28	270831.92	24063	129.81	353.81	8	13.06	265559.76	22538	124.4	334.63	8	12.26
	M3	365308.21	31395	171.65	464.26	11	16.86	389170.72	34771	187.08	510.70	11	17.49	357800.20	31665	170.96	465.76	11	16.70	365180.53	30021	168.44	448.89	11	16.44
	L1	791357.29	57747	350.72	894.17	16	40.79	782633.89	60278	355.41	921.08	16	39.19	812023.11	59784	364.15	926.93	16	39.46	765692.29	55157	339.18	858.89	16	41.40
	L2	949506.48	70540	427.15	1090.82	21	51.98	991180.12	75926	452.66	1165.92	21	50.70	945550.06	70648	427.16	1091.74	21	56.60	952795.68	69983	425.66	1084.37	21	51.71
	L3	1135763.90	82678	506.25	1284.95	26	63.735	1139216.20	88359	525.10	1354.91	26	62.18	1152256.40	86819	521.53	1337.72	26	61.42	1139656.40	83981	513.45	1304.30	26	61.40
	Average	364557.56	28147.82	165.21	429.25	9	18.27	369688.68	29827.91	171.44	450.70	9	17.99	367383.2	28893.64	168.33	439.18	9	18.34	361182.01	**27722.27**	163.72	423.92	9	18.02
Fuel Consumption	S1	28268.68	2535	13.11	36.63	1	0.65	27728.87	2565	13.14	36.91	1	0.55	28239.25	2689	13.65	38.56	1	0.56	27557.55	2679	13.47	38.26	1	0.58
	S2	43303.85	3971	20.54	57.3724	2	1.07	45663.87	4446	22.38	63.52	2	1.15	45038.12	4392	22.12	62.77	2	1.07	43184.99	4333	21.61	61.68	2	1.07
	S3	50340.76	4711	24.16	67.8214	2	1.38	48312.55	4913	24.39	69.81	2	1.38	49684.01	5039	25.06	71.65	2	1.34	48276.76	4790	23.98	68.29	2	1.40
	S4	56684.72	5416	27.38	77.52	3	1.81	56930.82	5910	28.98	83.56	3	1.81	64412.77	6304	31.48	89.79	3	1.88	57403.19	5934	29.07	83.86	3	1.85
	S5	66279.16	6245	31.91	89.77	3	2.26	72336.26	7102	35.653	101.37	3	2.29	66895.16	6549	32.92	93.53	3	2.23	67149.44	6655	33.26	94.82	3	2.26
	M1	216729.08	20216	105.67	293.36	6	10.13	224435.65	21775	111.61	313.44	6	10.16	219218.81	20736	107.66	300.07	6	10.17	214083.06	19889	104.87	289.66	6	9.97
	M2	263651.68	25379	130.83	366.17	8	15.33	263994.67	26084	132.55	374.14	8	15.27	260370.51	25132	128.97	361.94	8	15.00	242653.86	23219	120.20	335.59	8	15.01
	M3	343197.35	32073	168.03	465.86	11	19.78	326875.12	32713	167.09	470.22	11	19.99	337824.65	31895	166.78	462.90	11	19.76	346888.29	31682	168.05	462.55	11	19.70
	L1	760586.21	59333	344.53	900.55	16	51.71	735637.12	61063	342.73	913.17	16	53.40	779393.06	63408	358.58	951.33	16	50.25	733733.37	59196	337.43	891.21	16	50.59
	L2	884681.06	71607	410.00	1080.16	21	65.82	910252.34	77263	432.43	1154.03	21	63.83	926827.54	75722	430.76	1139.01	21	63.32	890330.51	73301	414.98	1100.29	21	63.22
	L3	1061703.2	85386	491.07	1290.52	26	80.35	1067284.70	90303	504.77	1348.06	26	79.04	1077163.70	88315	503.53	1329.74	26	78.75	1092351.10	87956	505.32	1328.74	26	78.83
	Average	**343220.52**	28806.55	160.66	429.61	9	22.75	**343586.54**	30376.09	**165.06**	448.02	9	22.62	**350460.69**	30016.45	165.59	445.57	9	22.21	**342146.56**	29057.64	**161.11**	432.27	9	22.22
Cost	S1	28590.28	2484	13.072	36.15	1	0.63	28778.85	2470	13.09	36.05	1	0.64	29509.17	2636	13.83	38.31	1	0.63	28596.47	2558	13.31	37.05	1	0.62
	S2	43448.91	3971	20.569	57.41	2	1.14	45707.28	4446	22.39	63.54	2	1.18	45434.61	4384	22.16	62.75	2	1.15	39327.56	3678	18.98	53.09	2	1.14
	S3	53645.44	4654	24.836	68.12	2	1.55	51874.55	4951	25.39	71.28	2	1.55	51059.78	4981	25.17	71.28	2	1.52	49893.00	4802	24.42	68.90	2	1.48
	S4	58800.72	5286	27.476	76.53	3	2.06	57960.88	5849	28.96	83.02	3	2.07	64930.74	6292	31.56	89.77	3	2.09	59000.68	5835	29.07	83.03	3	1.89
	S5	69397.56	6299	32.642	91.08	3	2.50	73734.26	7061	35.78	101.16	3	2.51	73979.65	6882	35.35	99.15	3	2.55	75254.39	6781	35.43	98.38	3	2.57
	M1	218607.40	19497	104.23	285.59	6	11.30	225560.02	20700	109.93	302.37	6	11.74	213804.99	19707	103.62	286.67	6	10.33	210175.53	18713	100.44	274.57	6	10.86
	M2	277086.37	25166	132.95	366.80	8	16.65	282782.19	26091	138.22	380.73	8	18.79	277440.83	24913	132.50	364.13	8	17.26	254759.73	22922	122.07	335.22	8	17.87
	M3	340510.47	30598	164.43	449.18	11	23.43	351031.59	32781	172.82	477.38	11	23.67	346698.40	31189	166.55	456.64	11	23.35	345371.96	30328	163.86	446.23	11	22.97
	L1	779854.70	57737	347.02	889.83	16	59.39	749278.21	59939	345.03	906.26	16	60.10	786083.18	59677	354.11	914.49	16	57.86	793413.91	58210	351.46	898.96	16	57.76
	L2	911031.30	69486	411.07	1063.36	21	75.05	912630.60	74141	424.05	1117.86	21	76.00	889145.04	70469	409.44	1069.85	21	73.45	910834.93	69534	412.11	1064.97	21	74.62
	L3	1066019.10	82704	487.95	1264.13	26	92.62	1099216.10	88976	513.49	1346.81	26	91.94	1115233.90	86046	509.99	1317.88	26	90.50	1105616.90	84137	501.23	1291.58	26	93.03
	Average	349726.57	**27989.27**	**160.57**	**422.56**	9	26.03	352595.87	**29764.09**	166.29	**444.22**	9	26.38	353938.21	**28834.18**	**164.02**	**433.72**	9	25.52	352022.28	27954.36	161.13	**422.91**	9	25.89

Table 7 reports the impact of demand size on travel time, fuel consumption and costs. In the light of these results, instances with large demand tend to be more expensive in terms of emission and operational costs compared to low or medium-size ones. Table 7 provides some insights on the impact of carried loads over the five performance measures. Results of the TDNNH are obtained under the three minimization criteria. As expected, the number routes increases when the volume of orders increases, which has a considerable impact on the level of fuel consumption and overall costs. For the cost minimization objective, both fuel consumption and cost doubled from 116.24 liters and 318.01$ (case of low demands) to 280 liters and 736.29$ (case of high demands). This behavior is coherent with the fact that, proportionally, fuel consumption increases as both load and the number of routes increase, on average, from 3.91 to 20.27. Additionally, we have noticed that fuel consumption increases by 43.06% (116.24 vs 166.29 liters) in the case of medium demand against 140.88% (116.24 vs 280 liters) for high demand one. A key finding is that combining heterogeneous loads (case of medium demand) could be beneficial in optimizing both fuel consumption and costs.

6 Conclusions

In this paper we have studied the Time-dependent Vehicle Routing Problem with Emission and Cost Minimization considering time-varying speeds and dynamic paths. In order to solve it, we have developed an efficient method combining a goal directed search heuristic, called Time-dependent Nearest Neighborhood heuristic (TDNNH) with a Time-dependent Neighborhood Search Improvement heuristic (TDNSIH). An efficient adaptation of the Dijkstra label-setting algorithm to a time-dependent setting is embedded into the solution methods to perform the fast computation of time-dependent point-to-point paths connecting pairs of customers nodes based on different measures, namely fuel consumption (TDLEP), time (TDQP) or cost (TDLCP) leading to a larger search space and further opportunities of optimization in large time-dependent road networks. The results of extensive computational experiments on real-life benchmark instances demonstrate that taking dynamic paths into account according to time-varying speeds yields good quality solutions in a very consistent manner using the TDNSIH, outperforming the classical SNNH with fixed speed limits. In fact, some routes that were evaluated as profitable can now appear as not viable candidates in the case of time-dependent network modeled as a multigraph which reflect more realistic scenarios.

Moreover, our analysis have shown that potential reduction in GHG emissions and costs are achievable through flexible departure times, which allows congestion avoidance considering alternative paths

Table 7: Impact of the variation in demand on the emissions of routes: average across TDVRP-ECMDP benchmark instances using the TDNNH

Optimization measure	Instances	Low demand					Medium demand					High demand				
		Dist	TT	Fuel	Cost	#Routes	Dist	TT	Fuel	Cost	#Routes	Dist	TT	Fuel	Cost	#Routes
Travel Time	S1	28992.49	2472	12.72	35.64	1	29259.33	2470	13.17	36.14	1	42626.35	3733	19.72	54.41	2
	S2	30962.95	2933	14.65	41.78	1	40001.63	3517	18.71	51.42	2	48052.05	4480	22.90	64.41	3
	S3	42113.26	3766	19.58	54.52	1	50780.25	4719	24.45	68.22	2	74419.39	6604	34.99	96.37	4
	S4	59307.18	5147	27.21	75.04	1	65390.99	6224	31.49	89.11	3	103226.39	9436	49.17	136.75	6
	S5	59314.43	5305	28.07	77.37	1	76327.99	7247	36.837	103.962	3	111835.09	10446	54.10	151.01	7
	M1	164008.87	15422	79.40	222.40	3	214312.95	19193	103.14	281.75	6	315950.70	28722	153.02	420.11	13
	M2	218106.04	20160	104.61	291.66	4	288301.37	25403	137.85	374.45	8	435925.17	38231	208.21	564.41	18
	M3	274611.38	25329	131.70	366.76	5	389170.72	34771	187.08	510.70	11	582756.17	51558	279.64	759.832	25
	L1	526368.51	41454	236.39	624.21	7	782633.89	60278	355.41	921.079	16	1323580.20	99727	599.26	1536.83	36
	L2	623879.88	51084	284.31	761.17	9	991180.12	75926	452.66	1165.92	21	1630572.70	124152	742.55	1909.22	48
	L3	714542.23	58942	331.31	882.01	10	1139216.20	88359	525.10	1354.91	26	2081732.70	158484	948.21	2437.56	61
	Average	249291.57	21092.18	115.45	312.05	3.91	369688.68	29827.91	171.45	450.70	9	613697.90	48688.45	282.89	739.17	20.27
Fuel Consumption	S1	27754.50	2526	12.62	35.98	1	27728.87	2565	13.14	36.91	1	40886.59	3784	19.46	54.5429	2
	S2	30960.31	2933	14.65	41.78	1	45663.87	4446	22.38	63.52	2	47578.51	4484	22.81	64.35	3
	S3	36824.82	3786	18.45	53.39	1	48312.55	4913	24.39	69.81	2	73882.84	6982	36.05	100.80	4
	S4	49569.13	4857	24.28	69.20	1	56930.82	5910	28.98	83.56	3	92940.35	9079	45.88	129.93	6
	S5	55676.97	5372	27.45	77.23	1	72336.26	7102	35.65	101.37	3	105710.78	10443	53.28	150.04	7
	M1	161858.78	16390	81.60	233.16	3	224435.65	21775	111.61	313.44	6	281374.75	27751	142.54	399.80	12
	M2	199829.99	20821	102.84	295.25	4	263994.67	26084	132.55	374.14	8	401711.55	39298	202.62	567.04	18
	M3	240960.33	24894	123.59	353.73	5	326875.12	32713	167.09	470.22	11	555849.38	52904	276.51	767.67	25
	L1	515976.69	44620	243.06	658.79	7	735637.12	61063	342.73	913.17	16	1277676.6	102856	592.24	1555.35	36
	L2	608081.81	54046	288.48	791.139	9	910252.34	77263	432.43	1154.03	21	1613860.5	133783	756.42	2007.04	48
	L3	679157.74	61334	324.93	895.004	11	1067284.70	90303	504.77	1348.06	26	1970353.5	162889	927.37	2451.03	61
	Average	236968.28	21961.73	114.72	318.60	4	343586.54	30376.09	165.06	448.02	9	587438.67	50386.64	279.56	749.78	20.18
Cost	S1	28728.49	2472	12.67	35.59	1	28778.85	2470	13.09	36.05	1	42236.93	3733	19.6	54.32	2
	S2	30960.31	2933	14.65	41.78	1	45707.28	4446	22.39	63.54	2	47578.51	4484	22.81	64.35	3
	S3	41336.73	3766	19.41	54.33	1	51874.55	4951	25.39	71.28	2	69933.53	6558	33.84	94.65	4
	S4	50953.14	4920	24.70	70.23	1	57960.88	5849	28.96	83.02	3	95368.84	9023	46.26	129.90	6
	S5	58066.54	5261	27.68	76.56	1	73734.26	7061	35.78	101.16	3	109621.49	10467	53.74	150.77	7
	M1	179326.06	16941	87.07	244.12	3	225560.02	20700	109.93	302.37	6	298359.01	27595	146.00	402.45	12
	M2	188471.62	18441	94.17	265.05	3	282782.19	26091	138.22	380.73	8	434687.07	37380	205.40	553.94	18
	M3	272926.74	26763	135.98	383.86	5	351031.59	32781	172.82	477.38	11	549997.86	48975	264.77	720.78	25
	L1	555539.51	44986	251.71	671.84	7	749278.21	59939	345.03	906.26	16	1324648.10	98306	598.40	1523.76	36
	L2	611756.63	51245	281.88	759.75	9	912630.60	74141	424.05	1117.86	21	1673384.10	126721	761.85	1953.26	49
	L3	693992.86	59617	328.73	884.78	11	1099216.10	88976	513.49	1346.81	26	2046900.60	152708	929.63	2367.09	61
	Average	246550.78	21576.82	116.24	317.08	3.91	352595.87	29764.09	166.29	444.22	9	601469.90	48739.18	280.00	736.29	20.27

between customers. Additionally, we have observed that the size of orders affects paths choice decision yielding different route plans with higher level of fuel consumption. Further research can now focus on generalizing these methods to broader distribution problems, namely the time-dependent inventory-routing and dynamic vehicle routing problems.

A CMEM parameters

We set the values of the CMEM input parameters based on the specification of Barth and Boriboonsomsin [2009] as follows: the curb-weight $\omega = 15000\ kg$, carried load q between 0-10000 kg, fuel-to-air mass ratio $\zeta = 1$, engine friction factor $k = 0.25\ kJ/rev/L$, engine speed $N_e = 60$, engine displacement $V = 7\ L$, gravitational constant $g = 9.81\ m/s^2$, air density $\rho = 1.2041\ k/m^3$, coefficient of aerodynamic drag $C_d = 0.7$, frontal surface area $A = 3.912\ m^2$, coefficient of rolling resistance $C_r = 0.01$, vehicle drive train efficiency $\eta_{tf} = 0.4$, efficiency parameter for diesel engines $\eta = 0.9$, fuel and GHG emissions cost per liters $c_f = 1.2$ \$CAD/liters, driver wage $c_d = 0.0085$ \$CAD/s, heating value of a typical diesel fuel $\varpi = 44\ kJ/g$, conversion factor from g/s to L/s $\psi = 737$, lower speed limit $s^l = 1.388\ m/s$, upper speed limit $s^u = 30.555\ m/s$, acceleration $a = 0\ m/s^3$, and roadway gradient $\theta = 0$ degree.

B Time-dependent Dijkstra label-setting algorithm

The TD-Dijkstra algorithm is applied to determine time-dependent paths by using a node-examination process considering time-varying speeds from an origin o to a destination d. A pseudocode is presented in Algorithm 4.

Algorithm 4 Time-dependent Dijkstra label-setting algorithm (TD-Dijkstra)

function TD_DIJKSTRA$(o, d, t, \mathcal{G}^{\mathcal{T}})$
  $\mathcal{E} \leftarrow \varnothing$, $\mathcal{N} \leftarrow \mathcal{V}^{\mathcal{T}}$, $predecessor(o) \leftarrow o$, $c_o \leftarrow 0$, $c_u \leftarrow \infty | \tau_u \leftarrow 0$, $\forall u \in \mathcal{V}^{\mathcal{T}}$
  while $|\mathcal{E}| < n$ **do**
    let $u \in \mathcal{N}$ be a node for which $c_u \leftarrow \min\{c_v : v \in \mathcal{N}\}$
    $\mathcal{E} \leftarrow \mathcal{E} \cup \{u\}$, $\mathcal{N} \leftarrow \mathcal{N} \backslash \{u\}$
    if $u = d$ **then**
      Stop
    end if
    $t \leftarrow t + \tau_u$
    for each $(u, v) \in \mathcal{E}_+^{\mathcal{T}}(u)$ **do**
      if $c_v > \left[TD\_Cost\_FSM(t, (u, v), \mathcal{Z}^{\mathcal{T}}) \longrightarrow c_{uv}(t)\right]$ **then**
        $c_v \leftarrow c_u + \left[TD\_Cost\_FSM(t, (u, v), \mathcal{Z}^{\mathcal{T}}) \longrightarrow c_{uv}(t)\right]$
        $\tau_v \leftarrow c_u + \left[TD\_Cost\_FSM(t, (u, v), \mathcal{Z}^{\mathcal{T}}) \longrightarrow \tau_{uv}(t)\right]$
        $predecessor(v) \leftarrow u$
      end if
    end for
  end while
end function

References

Konstantinos N Androutsopoulos and Konstantinos G Zografos. An integrated modelling approach for the bicriterion vehicle routing and scheduling problem with environmental considerations. *Transportation Research Part C: Emerging Technologies*, 82:180–209, 2017.

Matthew Barth and Kanok Boriboonsomsin. Real-world carbon dioxide impacts of traffic congestion. *Transportation Research Record: Journal of the Transportation Research Board*, 2058:163–171, 2008.

Matthew Barth and Kanok Boriboonsomsin. Energy and emissions impacts of a freeway-based dynamic eco-driving system. *Transportation Research Part D: Transport and Environment*, 14(6):400–410, 2009.

Martin Behnke and Thomas Kirschstein. The impact of path selection on GHG emissions in city logistics. *Transportation Research Part E: Logistics and Transportation Review*, 106:320–336, 2017.

Tolga Bektaş and Gilbert Laporte. The pollution-routing problem. *Transportation Research Part B: Methodological*, 45 (8):1232–1250, 2011.

Khaled Belhassine, Leandro C Coelho, Jacques Renaud, and Jean-Philippe Gagliardi. Improved home deliveries in congested areas using geospatial technology. Technical Report CIRRELT-2018-02, Montreal, Canada, 2018.

Gerth Stølting Brodal and Riko Jacob. Time-dependent networks as models to achieve fast exact time-table queries. *Electronic Notes in Theoretical Computer Science*, 92:3–15, 2004.

Tobia Calogiuri, Gianpaolo Ghiani, and Emanuela Guerriero. The time-dependent quickest path problem: Properties and bounds. *Networks*, 66(2):112–117, 2015.

Said Dabia, Emrah Demir, and Tom Van Woensel. An exact approach for a variant of the pollution-routing problem. *Transportation Science*, 51(2):607–628, 2017.

Brian C Dean. Shortest paths in fifo time-dependent networks: Theory and algorithms. Technical report, Massachusetts Institute of Technology, 2004.

Frank Dehne, Masoud T Omran, and Jörg-Rüdiger Sack. Shortest paths in time-dependent FIFO networks. *Algorithmica*, 62(1-2):416–435, 2012.

Daniel Delling and Giacomo Nannicini. Core routing on dynamic time-dependent road networks. *INFORMS Journal on Computing*, 24(2):187–201, 2012.

Emrah Demir, Tolga Bektaş, and Gilbert Laporte. An adaptive large neighborhood search heuristic for the pollution-routing problem. *European Journal of Operational Research*, 223(2):346–359, 2012.

Emrah Demir, Tolga Bektaş, and Gilbert Laporte. The bi-objective pollution-routing problem. *European Journal of Operational Research*, 232(3):464–478, 2014a.

Emrah Demir, Tolga Bektaş, and Gilbert Laporte. A review of recent research on green road freight transportation. *European Journal of Operational Research*, 237(3):775–793, 2014b.

Marco Di Bartolomeo, Enrico Grande, Gaia Nicosia, and Andrea Pacifici. Cheapest paths in dynamic networks. *Networks*, 55(2):23–32, 2017.

Jan Fabian Ehmke, Ann Melissa Campbell, and Barrett W Thomas. Data-driven approaches for emissions-minimized paths in urban areas. *Computers & Operations Research*, 67:34–47, 2016a.

Jan Fabian Ehmke, Ann Melissa Campbell, and Barrett W Thomas. Vehicle routing to minimize time-dependent emissions in urban areas. *European Journal of Operational Research*, 251(2):478–494, 2016b.

Miguel Andres Figliozzi. The impacts of congestion on time-definitive urban freight distribution networks CO_2 emission levels: Results from a case study in Portland, Oregon. *Transportation Research Part C: Emerging Technologies*, 19 (5):766–778, 2011.

Bernhard Fleischmann, Martin Gietz, and Stefan Gnutzmann. Time-varying travel times in vehicle routing. *Transportation Science*, 38(2):160–173, 2004.

Anna Franceschetti, Dorothée Honhon, Tom Van Woensel, Tolga Bektaş, and Gilbert Laporte. The time-dependent pollution-routing problem. *Transportation Research Part B: Methodological*, 56:265–293, 2013.

Anna Franceschetti, Emrah Demir, Dorothée Honhon, Tom Van Woensel, Gilbert Laporte, and Mark Stobbe. A metaheuristic for the time-dependent pollution-routing problem. *European Journal of Operational Research*, 259(3):972–991, 2017.

Thierry Garaix, Christian Artigues, Dominique Feillet, and Didier Josselin. Vehicle routing problems with alternative paths: An application to on-demand transportation. *European Journal of Operational Research*, 204(1):62–75, 2010.

Michel Gendreau, Gianpaolo Ghiani, and Emanuela Guerriero. Time-dependent routing problems: A review. *Computers & Operations Research*, 64:189–197, 2015.

Gianpaolo Ghiani and Emanuela Guerriero. A lower bound for the quickest path problem. *Computers & Operations Research*, 50:154–160, 2014a.

Gianpaolo Ghiani and Emanuela Guerriero. A note on the Ichoua, Gendreau, and Potvin (2003) travel time model. *Transportation Science*, 48(3):458–462, 2014b.

H. Heni, L. C. Coelho, and J. Renaud. Time-dependent quickest path problem with emission minimization. Technical Report CIRRELT-2017-62, Montreal, Canada, 2017.

John Hickman, Dieter Hassel, Robert Joumard, Zissis Samaras, and S Sorenson. Methodology for calculating transport emissions and energy consumption. In *European Commission, DG VII. Technical Report*. 1999. URL `http://www.transport-research.info/sites/default/files/project/documents/meet.pdf`. Available online (accessed on February 17, 2018).

Yixiao Huang, Lei Zhao, Tom Van Woensel, and Jean-Philippe Gross. Time-dependent vehicle routing problem with path flexibility. *Transportation Research Part B: Methodological*, 95:169–195, 2017.

Soumia Ichoua, Michel Gendreau, and Jean Yves Potvin. Vehicle dispatching with time-dependent travel times. *European Journal of Operational Research*, 144(2):379–396, 2003.

O Jabali, T Van Woensel, and A.-G. de Kok. Analysis of travel times and CO_2 emissions in time-dependent vehicle routing. *Production and Operations Management*, 21(6):1060–1074, 2012.

Adrianus Leendert Kok, EW Hans, and JMJ Schutten. Vehicle routing under time-dependent travel times: the impact of congestion avoidance. *Computers & Operations Research*, 39(5):910–918, 2012.

Raphael Kramer, Nelson Maculan, Anand Subramanian, and Thibaut Vidal. A speed and departure time optimization algorithm for the pollution-routing problem. *European Journal of Operational Research*, 247(3):782–787, 2015a.

Raphael Kramer, Anand Subramanian, Thibaut Vidal, and F Cabral Lucídio dos Anjos. A matheuristic approach for the pollution-routing problem. *European Journal of Operational Research*, 243(2):523–539, 2015b.

David SW Lai, Ozgun Caliskan Demirag, and Janny MY Leung. A tabu search heuristic for the heterogeneous vehicle routing problem on a multigraph. *Transportation Research Part E: Logistics and Transportation Review*, 86:32–52, 2016.

Adam N Letchford, Saeideh D Nasiri, and Amar Oukil. Pricing routines for vehicle routing with time windows on road networks. *Computers & Operations Research*, 51:331–337, 2014.

Jiani Qian and Richard Eglese. Fuel emissions optimization in vehicle routing problems with time-varying speeds. *European Journal of Operational Research*, 248(3):840–848, 2016.

Kiseok Sung, Michael GH Bell, Myeongki Seong, and Soondal Park. Shortest paths in a network with time-dependent flow speeds. *European Journal of Operational Research*, 121(1):32–39, 2000.

Éric Taillard, Philippe Badeau, Michel Gendreau, François Guertin, and Jean-Yves Potvin. A tabu search heuristic for the vehicle routing problem with soft time windows. *Transportation Science*, 31(2):170–186, 1997.

Hamza Ben Ticha, Nabil Absi, Dominique Feillet, and Alain Quilliot. Empirical analysis for the VRPTW with a multigraph representation for the road network. *Computers & Operations Research*, 88:103–116, 2017.

Transports Canada. Transportation in Canada 2016. `https://www.tc.gc.ca/media/documents/policy/comprehensive_report_2016.pdf`, 2017. Available online (accessed on February 17, 2018).

Tom Van Woensel, Laoucine Kerbache, Herbert Peremans, and Nico Vandaele. Vehicle routing with dynamic travel times: A queueing approach. *European Journal of Operational Research*, 186(3):990–1007, 2008.

L. Wen, B. Çatay, and R. Eglese. Finding a minimum cost path between a pair of nodes in a time-varying road network with a congestion charge. *European Journal of Operational Research*, 236(3):915–923, 2014.

Yiyong Xiao and Abdullah Konak. The heterogeneous green vehicle routing and scheduling problem with time-varying traffic congestion. *Transportation Research Part E: Logistics and Transportation Review*, 88:146–166, 2016.

Emmanouil E Zachariadis and Chris T Kiranoudis. A strategy for reducing the computational complexity of local search-based methods for the vehicle routing problem. *Computers & Operations Research*, 37(12):2089–2105, 2010.